Bulk Metallic Glasses for Biomedical Applications

Jan Schroers, Golden Kumar, Thomas M. Hodges, Stephen Chan, and Themis R. Kyriakides

The selection criteria for biomaterials include the material's properties and biocompatibility, and the ability to fabricate the desired shapes. Bulk metallic glasses (BMGs) are relative newcomers in the field of biomaterials but they exhibit an excellent combination of properties and processing capabilities desired for versatile implant applications. To further evaluate the suitability of BMGs for biomedical applications, we analyzed the biological responses they elicited in vitro and in vivo. The BMGs promoted cell adhesion and growth in vitro and induced improved foreign body responses in vivo suggesting their potential use as biomaterials. Because of the BMGs' flexible chemistry, atomic structure, and surface topography, they offer a unique opportunity to fabricate complex implants and devices with a desirable biological response from a material with superior properties over currently used metallic biomaterials.

INTRODUCTION

The availability and suitability of traditional materials for bio-prosthetic elements are limited. As a result, significant interest has been drawn to developing synthetic materials, which promise asymptomatic, long-term use within the body. Material choice is defined by the function of the implant and the material's compatibility with the body's internal environment. Furthermore, the selection of an implant material also depends on its ability to be fabricated into a desired shape. Current biomaterials include a wide range of natural and manufactured materials such as ceramics, metals, and both synthetic polymers and biopolymers. Each type of material has its own positive aspects that are particularly suited for specific applications.

The use of metals in biomedical applications dates back to the 16th century, when Petronius used gold plates for the repair of cleft palates.[1] A high elastic modulus and yield strength coupled with ductility make metals suitable for bearing large loads without excessive deformation and permanent dimensional changes. Metallic implants are mainly used as prostheses to replace a missing body part and as fixation devices to stabilize bones and tissues during the healing process. Metals and alloys that are successfully used as biomaterials include steels, titanium-based alloys, Ni-Ti (shape memory alloy), cobalt-based alloys, and precious metal alloys. However, usage of metallic implant materials is limited by complex fabrication methods, which restrict design options, and also by their reduced long-term stability in corrosive environments. Therefore, the vast majority of bioengineering applications would benefit from the availability of a biomaterial with high corrosion and wear resistance, high strength and elasticity, and the ability to be net-shaped into intricate geometries.

How would you…

…describe the overall significance of this paper?

This article evaluates how bulk metallic glasses (BMGs), a new material class of structural metals with outstanding mechanical properties, can be used in biomedical implants and devices. The evaluation includes the introduction of recently developed processing methods which can be utilized to precision net-shape complex geometries.

…describe this work to a materials science and engineering professional with no experience in your technical specialty?

The absence of grain boundaries, dislocation, and associated slip planes results in BMGs with unusual properties. Their high strength and elasticity, exceeding that of currently used biomaterials, together with good wear and corrosion resistance are attractive properties as a biomaterial. Most unique is the processability of BMGs. They can be thermoplastically formed, similar to plastics, which permits precision net-shaping of complex geometries. This, together with biocompatibility tests on some BMGs propose a wide range of applications of BMG as biomedical implants and devices.

…describe this work to a layperson?

Bulk metallic glass, a novel material with amorphous structure which is a high strength metal that can be formed like a plastic, is evaluated for biomedical implants and devices. Biocompatibility tests have revealed that some BMGs can be used in the human body.

BULK METALLIC GLASSES

Bulk metallic glasses (BMGs) are metallic alloys which possess a particular ease to avoid crystallization during solidification and thereby vitrify at low cooling rates. Bulk metallic glasses have attracted much attention due to their remarkable properties like high strength, elasticity, corrosion resistance, and unique processing capabilities.[2–5] During the past two decades, a wide range of BMG-forming alloys has been developed, including Zr-,[6–8] Fe-,[9,10] Cu-,[11] Ni-,[12] Ti-,[13] Mg-,[14] Pd-,[15] Au-,[16] and Pt-based.[17] The unusual properties of BMGs are to a large extent a consequence of their amorphous structure. The absence of dislocations and associated slip-planes in BMGs results in a very high strength and elasticity close to the theoretical limit. For example, a typical zirconium-based BMG yields at 2,000 MPa with an elastic strain of

2%,[2] while currently used titanium-based biomaterials yield below 800 MPa at an elastic strain of 0.7%.[18]

In addition, BMGs are isotropic and homogeneous on small length scales, a property that becomes increasingly important when one dimension of an implant approaches the grain size in crystalline materials. Recently, it was demonstrated that BMGs show better corrosion properties in physiological solutions compared to many common metallic biomaterials, a result which is attributed to the absence of grain boundaries in the homogenous amorphous structure of BMGs.[19] Despite their desirable properties as a biomaterial only limited work has been carried out to characterize the biocompatibility of BMGs. Some recent work, however, suggests that some BMGs can support cell growth in vitro.[20,21]

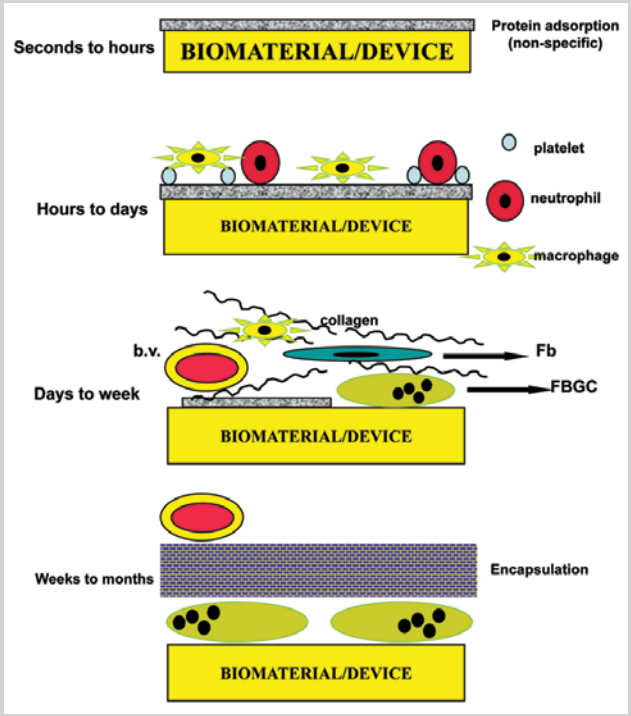

Figure 1. Development of the foreign body response. Implants acquire a proteinaceous coat within seconds to minutes following implantation. Subsequently, neutrophils and then macrophages adhere to the coated surface. Within a week, signals released from macrophages stimulate migration and extracellular matrix production by repair cells such as fibroblasts leading to encapsulation of the implant, a process that takes 2–4 weeks to stabilize. Formation of blood vessels is limited and such structures are infrequent in the mature foreign body response.

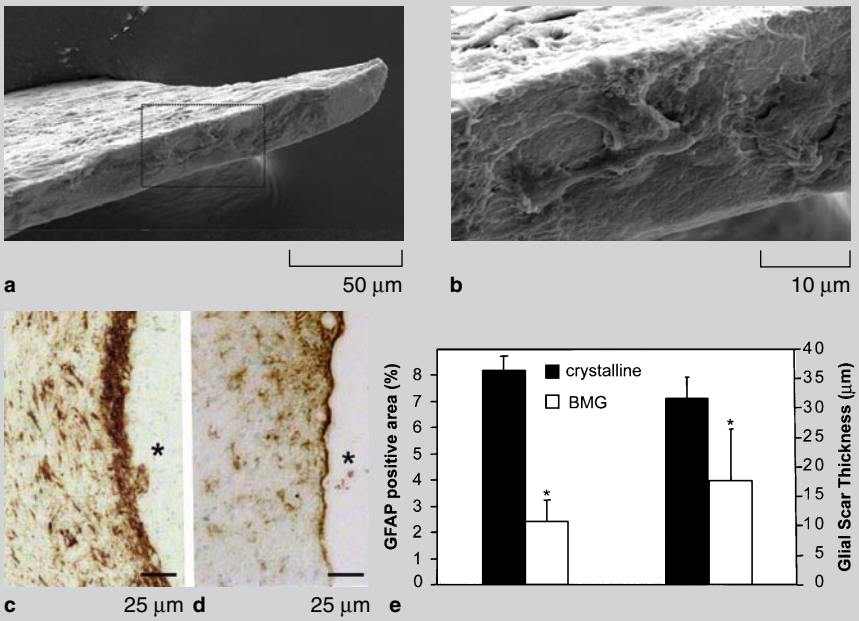

Figure 2. Foreign body response to BMGs. Representative scanning electron microscopy (a) low- and (b) high-magnification images of explanted BMGs 8 weeks following implantation in the brain are shown. Adherent proteinaceous material and cells can be observed on the surface of the implant. Representative images of sections stained with anti-GFAP antibodies and visualized with the peroxidase reaction (brown color) from brains that received (c) crystalline and (d) BMG implants. (*) in c and d denotes the location of the implant. (e) GFAP-positive area (expressed as % area) was evaluated by morphometric analysis of stained sections. Glial scar thickness (expressed in μm) was quantified with the aid of optical calipers. *p value <0.05.

BIOCOMPATIBILITY OF METALS

Of the three classes of materials commonly used for biomedical applications (ceramics, metals, and polymers), metals are the most commonly used. In general, metals possess attractive mechanical properties and exhibit natural biocompatibility. The latter implies that their interactions with cells and tissues do not elicit undesirable responses that

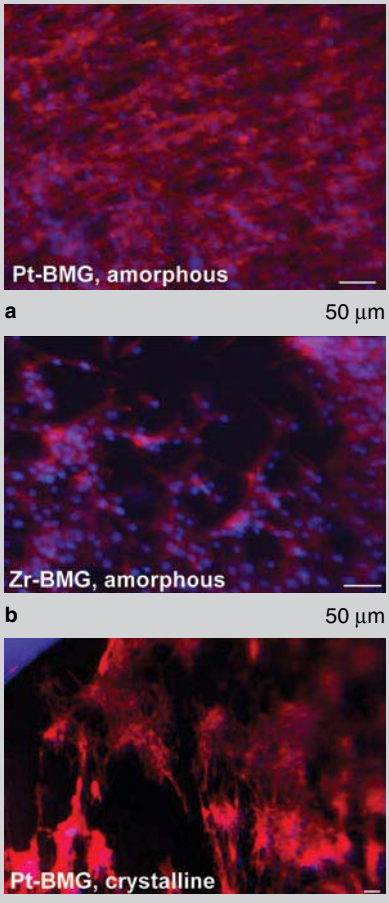

Figure 3. Normal cell growth on amorphous and crystallized BMGs. NIH3T3 fibroblasts were cultured on disks made of BMG materials for 48 h. Representative images of cells stained with rhodamine-phalloidin (red cytoskeleton) and DAPI (blue, nuclei) grown on (a) Pt-based BMG, (b) Zr-based BMG, and (c) crystallized Pt-based BMG are shown.

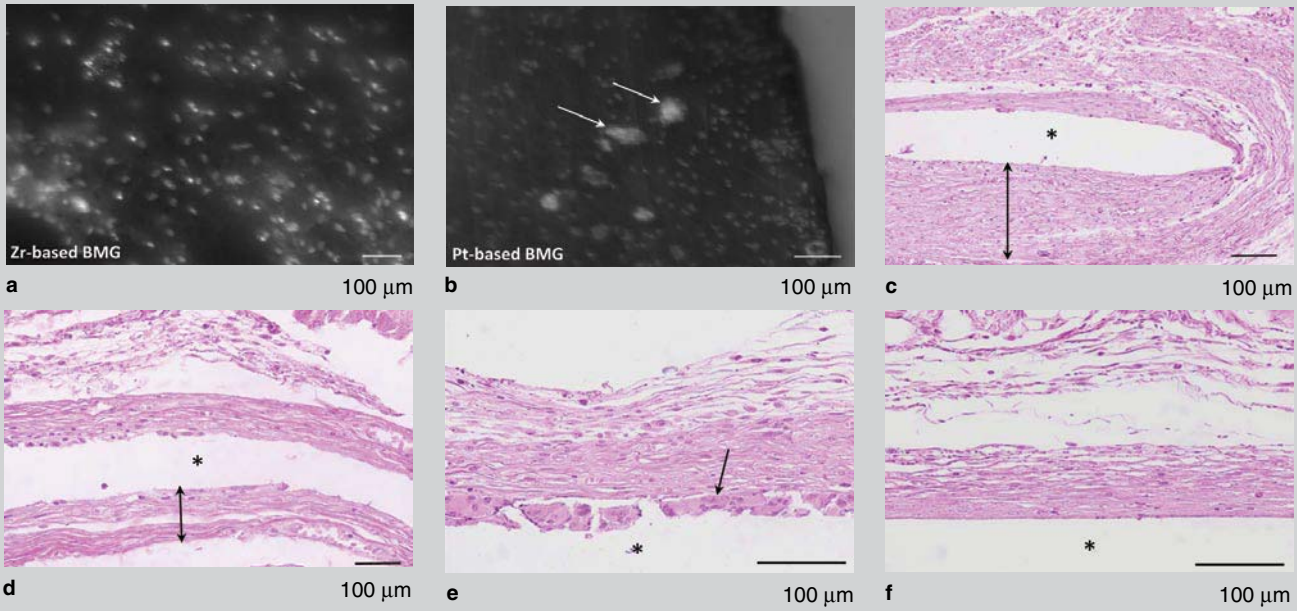

Figure 4. Foreign body response elicited by BMGs. Representative images of retrieved (a) Zr-based BMG and (b) Pt-based BMG stained with DAPI to visualize adherent cells after implantation. Arrows in (b) suggest the presence of FBGC. (c, d). Low and (e, f) high magnification images of (c, d) Zr-based and (d–f) Pt-based BMG implantation sites (*) stained with H&E. Double-sided arrows in (c) and (d) identify the collagenous capsule, which is thicker in response to Zr-based BMG. Arrow in (e) indicates the presence of FBGC.

could hinder their long-term function as implants. A recent review highlighted the importance of metal surface chemistry and biocompatibility.[22] Our current understanding, shown in Figure 1, of tissue-biomaterial interactions includes the following overlapping events: nonspecific protein adsorption, recruitment and adhesion of inflammatory cells, and recruitment of repair cells and remodeling of the implantation site leading to encapsulation of the implant. Animal studies are commonly used to evaluate these processes as they are elicited with test biomaterials. Moreover, in vitro studies are utilized to evaluate the effect of test biomaterials on cell viability and growth. Many factors, including the chemical and physical nature of the material as well as the type of tissue and duration of implantation, contribute to the overall biocompatibility. Specifically, materials chemistry, atomic structure, and surface topography can influence biocompatibility. Bulk metallic glass formers provide the unique opportunity to evaluate separately the influences of these factors. Therefore we considered two BMG formers, $Zr_{44}Ti_{11}Cu_{10}Ni_{10}Be_{25}$ (Zr-BMG)[23] and $Pt_{57.5}Cu_{14.7}Ni_{5.3}P_{22.5}$ (Pt-BMG)[17] BMGs, through in vitro and in vivo assays in their amorphous as well as crystalline states, with a variety of surface topographies.

In Vitro Cellular Responses

NIH 3T3 fibroblasts were cultured in DMEM supplemented with 10% fetal bovine serum and antibiotics. 1×10^5 cells were plated on disks (6 mm diameter) made of either $Zr_{44}Ti_{11}Cu_{10}Ni_{10}Be_{25}$ or $Pt_{57.5}Cu_{14.7}Ni_{5.3}P_{22.5}$ BMGs in 24-well

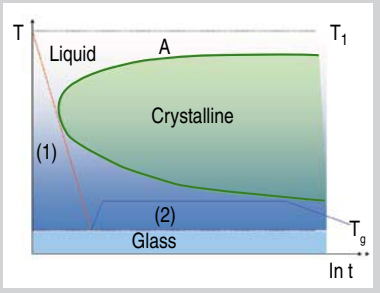

a

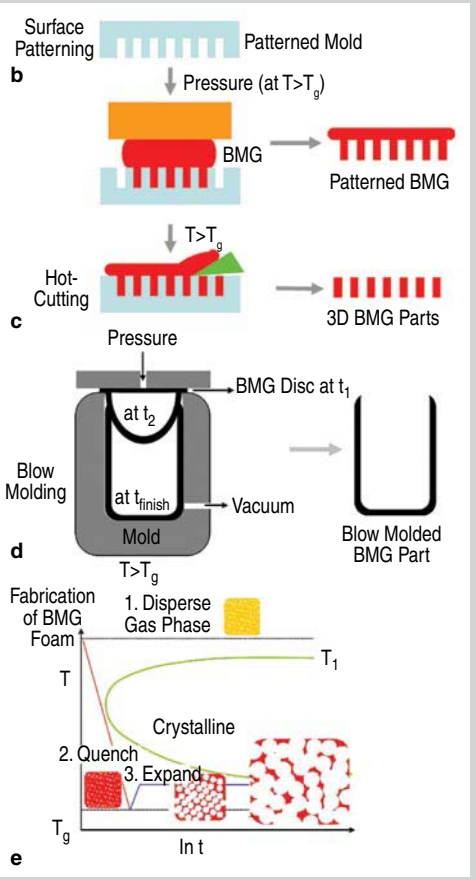

Figure 5. Processing of BMG former: (a) Schematic time-temperature-transformation (TTT) diagram indicating the two principle processing paths: (1) direct casting, where cooling and forming are carried out simultaneously and (2) thermoplastic forming, where the required fast cooling and forming are decoupled. (b–e) Schematic illustration of BMG processing methods based on TPF: (b) surface patterning by hot embossing, combined with (c) hot-cutting to make 3-D parts, (d) blow molding, and (e) fabrication of porous BMGs.

tissue culture plates for 48 h. Cells were fixed with 4% paraformaldehyde and stained with rhodamine-phalloidin and DAPI (Sigma) for 30 min. in the presence of 0.5% TritonX-100. Disks were washed with PBS and examined with the aid of an Olympus fluorescence microscope. Three different surface morphologies were considered on amorphous and crystalline alloys and the compatibility studies were repeated twice.

Foreign Body Response

All animal studies were approved by the Institutional Animal Care and Committee of Yale University. Alloy disks (6 mm in diameter and 0.2 mm thick) were implanted subcutaneously as described previously.[24] Briefly, sterile disks were inserted into the dorsal region of 3-mold C57Bl6 mice through a midline incision. Each mouse received two implants placed 1.5 cm apart. A total of three implants per type were evaluated. The incision was closed with surgical staples, which were removed at 2 weeks. Implants were excised en bloc at 4 weeks and then gently retrieved from the implantation site with forceps. Implants were fixed in 4% paraformaldehyde and stained with DAPI as described above. Tissues were fixed in formalin and processed for histological analysis. Sections were stained with hematoxylin and eosin and examined with the aid of a Nikon Eclipse microscope. Capsule thickness was evaluated by measuring twelve random areas of the capsule per section and a total of ten sections per implant.

In a separate study, alloy tapered strips (4 mm long, 1–2 mm wide, 50 μm thick) were implanted in the brain cortex of mice for a period of 8 weeks as described previously.[25] Prior to implant removal, brains were perfusion fixed to preserve the implantation site. Scanning electron microscopy analysis of explanted alloys revealed the accumulation of proteinaceous coat and numerous cells on the surface (Figure 2c–d). This suggests the strong adhesion of proteins and cells to the implant, which was similar between crystalline and BMG alloys. In addition, sections from brain tissues were stained with anti-GFAP antibodies (Zymed Laboratories; 1:50) to evaluate the extent of gliosis. Glia fibrillar acidic protein (GFAP) is expressed by astrocytes in the brain following injury and its accumulation is indicative of glial scarring, which is a consequence of injury that damages neural material. Both the GFAP-positive percent area and thickness of the gliotic scar were reduced in mice that received amorphous BMG implants compared to the crystalline form as shown in Figure 2c–e. The improved response of the amorphous BMG former might be due to the increased elasticity of the amorphous phase, which could reduce micromotion-associated injury to brain tissue.

Cellular Responses to BMGs

Platinum-based and zirconium-based alloys in their amorphous and crystalline states were evaluated for their ability to support cell growth. Different surface finishes ranging from rough (Ra ≈ 25–250 nm) to mirror polished were created to evaluate the influence of surface topography on the cell growth. As shown in Figure 3a, NIH3T3 fibroblasts displayed monolayer formation and firm attachment on the platinum-based BMG over a period of 48 h. Cells grew equally well on zirconium-based BMG (Figure 3b) and crystallized Pt-BMG (Figure 3c), but the cell monolayers lifted off during fixation and staining, suggesting that the cell attachment was suboptimal on both alloys in their crystalline state. Visualization of the cell cytoskeleton with rhodamine-phalloidin indicated normal fibroblast morphology and spreading. These findings are indistinguishable from our previously published results showing growth of fibroblasts on modified silicone.[26] In addition, elution assays, performed by incubating BMGs in media for 48 h and then adding the media to cells, revealed no negative effects on cell growth (not shown). Surface topography studies on the cell adhesion on the BMG material revealed that a rougher, 250 nm random roughness surface leads to better cell adhesion than a smooth (mirror finished) surface, in agreement with previous findings.[27–29]

Alloys were also evaluated in vivo following subcutaneous implantation in mice for a period of 4 weeks in order to allow for the full development of the foreign body response (FBR). It should be noted, however, that at this point, the breakdown of BMGs and release of individual metal components is not expected. Microscopic examination of retrieved implants stained with DAPI with a fluorescence equipped microscope revealed numerous adherent cells, including clusters of nuclei possibly representing foreign body giant cells (FBGC) (Figure 4). Such formations are common with all implanted biomaterials. Histological analysis of implantation sites indicated normal FBR including FBGC formation and encapsulation. The latter was characterized by deposition of collagen fibers and lacked extensive vascularization, which is typical. In comparison to platinum-based BMG, capsules surrounding zirconium-based BMG implants were thicker (112 ± 28 vs 178 ± 35 μm; p value ≤ 0.05; n = 3). Our findings are consistent with those obtained with biocompatible materials such as silicone and mixed cellulose ester filters, suggesting that platinum-based BMGs elicit a normal FBR.[30,31] In addition, we did not detect differences based on the surface finish of the two alloys suggesting that changes in the surface microarchitecture did not influence the FBR. Based on our in vitro and in vivo analysis, we conclude that BMGs induce normal biological responses and could be used as biomaterials or as components of implantable devices.

Though the in vivo and in vitro tests indicate that the BMGs tested in the present paper are in general non-toxic to cells, new BMGs are being explored to avoid toxic beryllium. Cytotoxicity is also attributed to nickel; however, shape memory alloys used in stents contain high nickel content. Studies on functionally graded Ni-Ti alloys have shown biocompatibility up to nickel content of about 50 wt.%.[32] The amount of nickel content in the present BMGs is less than 10 wt.%. Additionally, coatings can be used to extend the potential of BMG implants containing nickel and copper. It has been reported that the coating of Ni-Ti alloys significantly reduces the nickel release.[33]

Fabrication Methods for BMGs

The main challenge associated with processing of BMGs is their metastable nature: fast cooling conditions are re-

quired to avoid crystallization during processing. This limits the range of geometries that can be cast, since filling of the mold and fast cooling (which require opposite conditions) must be carried out simultaneously.[3] The solution to this problem is the emergence of thermoplastic forming (TPF) of BMGs in their supercooled liquid region (SCLR). During TPF the fast cooling to vitrify the BMG is decoupled from the molding operation.

The fabrication of BMGs using direct casting and TPF is compared in the schematic time-temperature-transformation (TTT) diagram shown in Figure 5a.[34] In both methods, crystallization during solidification must be avoided, as a BMG alloy in its crystalline state can no longer be formed, and its mechanical properties are significantly degraded.[35] Crystallization sets in when the processing temperature-time profile intersects with the crystallization curve (see Figure 5a). During direct casting, the crystallization nose must be bypassed while simultaneously filling the mold cavity. This is challenging, and only a careful balance of processing parameters permits one to net-shape some limited geometries with acceptable surface finish and residual stresses.[3] In addition, heterogeneous impurities in the material or the processing environment were also found to affect the crystallization kinetics significantly at temperatures above the nose of the TTT diagram.[36] As a consequence, the cooling protocol used in a fabrication process might result in either amorphous or (partially) crystalline material, leaving this fabrication process highly unpredictable. The limited geometrical range and the unpredictability of the casting process has prevented the widespread use of BMGs in the past.

Within the alternative TPF process, fast cooling required to avoid crystallization during solidification is decoupled from shaping, yielding advantages in geometrical range and accuracy. Furthermore, below the nose, where TPF is carried out, the influence of heterogeneities on the crystallization vanish, suggesting a predictable process which is insensitive to environmental influences.[36,37] For TPF, amorphous feedstock is produced through direct casting into simple shapes (path 1 in Figure 5a). During the TPF, this feedstock is heated to a temperature in the SCLR, where the BMG significantly softens and can be shaped under a low applied pressure. Recently developed alloys, $Pt_{57.3}Cu_{14.6}Ni_{5.3}P_{22.8}$,[17] $Zr_{44}Ti_{11}Cu_{10}Ni_{10}Be_{25}$,[23] $Zr_{40}Ti_{25}Cu_{25}Be_{10}$,[38] and $Au_{49}Ag_{5.5}Pd_{2.3}Cu_{26.9}Si_{16.3}$,[39] were specifically formulated for TPF, and their forming pressures and temperatures are comparable to those used for plastic processing.[3,38,40,41] These BMGs can be processed via TPF at low temperatures and pressures, and can be slowly cooled after processing resulting in BMG parts with negligible shrinkage and associated stresses. As a consequence, the dimensional accuracy of thermoplastically fabricated BMG parts is outstanding.[34]

Figure 5b–e shows a schematic illustration of various processing methods based on TPF. For surface patterning (Figure 5b), the BMG is placed on the patterned mold and heated to a temperature in the SCLR. The patterned molds can be fabricated from essentially any material with sufficient strength at the forming temperature including silicon, alumina, nickel, SU8, or even another BMG with different softening characteristics. Pressure exceeding the flow stress of BMG is applied to fill the BMG into the mold pattern. The flow stress of BMGs typically reduces to 0.1–10 MPa in the SCLR,[42] allowing them to deform by ~1,000% under low pressures. Following the forming process, the embossed BMG is separated from the mold, either mechanically or by etching, depending on the complexity of the mold pattern. The inverted replica of the mold pattern is imprinted on the BMG surface resulting in patterned BMGs as shown in Figure 5b. This process can also be combined with a hot-cutting method to fabricate three-dimensional (3-D) BMG components.[43] The mold filled with BMG is reheated into the SCLR and the BMG "reservoir" is scraped off the mold, as schematically illustrated in Figure 5c. After scraping, the 3-D miniature BMG parts are released by etching.

It has been recently demonstrated that the low forming pressure of some BMGs can be utilized for blow molding.[44] Even a pressure exerted by the human lung alone is sufficient to deform (>100%) the BMG in the SCLR.[44] This blow molding can be further combined with molding to net-shape geometries that are challenging or even impossible by conventional metal processing techniques. A schematic of the setup to use the blow mold ability as a net-shape process is shown in Figure 5d. Bulk metallic glass discs of about 1 mm thickness are used as feedstock material. The entire setup is heated to a temperature in the SCLR. A pressure difference between the top and the bottom side of the disc is applied to form the BMG into the mold shape. With increasing processing time from t_1 to t_2 the BMG disc deforms freely in the beginning and eventually conforms to the shape of mold at t_{finish}. The advantage of using blow molding over conventional molding is that the BMG is significantly deformed before coming in physical contact with mold. This reduces the friction (i.e., maximizes the achievable deformation). For example, large thin sections with high aspect ratio are challenging to fabricate using the embossing process described in Figure 5b and c due to friction between the mold and BMG.

The unique softening of BMGs in the SCLR can also be utilized to synthesize porous BMGs. It has been recently demonstrated that porous foam can be expanded in the SCLR when the environment pressure is reduced below the pressure in the porous material.[45–47] This finding is the basis of the proposed three-step synthesis process, which is sketched in Figure 5e. In the first step gas or a gas-releasing agent (GRA) is dispersed into the BMG-forming alloy. This mixture is fast cooled to render its amorphous state during solidification. In the next processing step the mixture is reheated into the SCLR where the environmental pressure is reduced below the pressure in the porous mixture to act as a driving force for expansion. Density of the porous BMG can be controlled by the expansion time.

BMG COMPONENTS FABRICATED BY TPF-BASED METHODS

Patterned Surfaces

Figure 6 shows scanning electron microscopy (SEM) images of BMGs patterned on different length scales

using the described surface patterning technique (Figure 5b). Figure 6a and b shows Pt-BMG embossed on porous alumina under pressure of 20 MPa at 250°C and 280°C, respectively. The alumina was dissolved in KOH solution resulting in patterned Pt-BMG surfaces. The diameter of the patterned features is about 100 nm and by changing embossing conditions the height of features can be varied. Figure 6b demonstrates that surface patterns can be extended into long hair-like fibers mimicking structures of sticky feet found in many insects and animals such as geckos, skinks, and tree frogs. Figure 6c and d shows the SEM images of Zr-BMG embossed at 430°C under 20 MPa on patterned silicon and nickel, respectively. Both Pt-BMG and Zr-BMG precisely replicate the mold patterns on length scales ranging from 20 nm to several hundred micrometers. It has been widely observed that the cellular response to an implant depends on the implant's chemistry and surface topography.[48–50] The surface pattern's length scale defines the interaction mechanism; for length scales <100 nm protein adsorption can be influenced[51] whereas for length scales >1 μm cell adhesion is controlled.[51,52] The ease in fabrication of controlled topographical features on BMGs can provide an access to a wide range of surface patterns that otherwise require complex microfabrication technology.

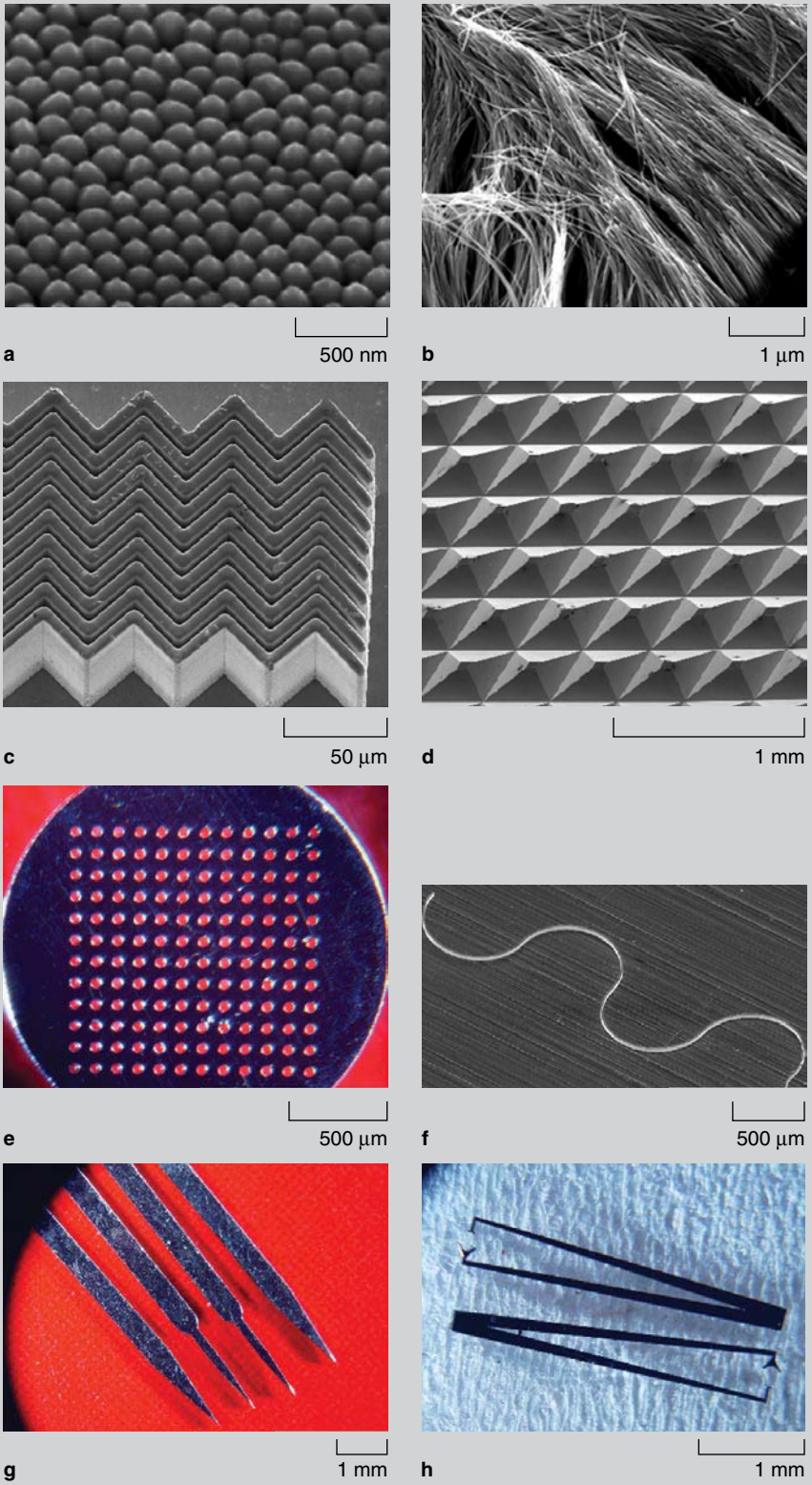

Figure 6. Miniature forming of BMGs: (a–d) SEM images of BMGs patterned by hot embossing of (a,b) Pt-BMG on porous alumina and (c) Zr-BMG on silicon mold, and (d) Zr-BMG on nickel mold. (e–h) Miniature $Zr_{44}Ti_{11}Cu_{10}Ni_{10}Be_{25}$ and $Pt_{57.5}Cu_{14.7}Ni_{5.3}P_{22.5}$ BMG parts that were created by TPF processes. Hot embossing was used to replicate the mold cavity and subsequent hot scraping to separate the BMG part from the forming reservoir.

MINIATURE PRECISION NET-SHAPING

Figure 6e–h shows images of free-standing BMG components fabricated using combined embossing and hot-separation processes as described in Figure 5b and c. Figure 6e is an optical micrograph of a Pt-BMG membrane with 50 μm diameter holes fabricated by embossing over silicon mold at 280°C for 100 s under a forming pressure of 20 MPa followed by hot cutting at the same temperature. The holes are well defined with sharp edges demonstrating the outstanding dimensional accuracy achieved by the TPF of BMGs in all three dimensions. Figure 6f shows an SEM image of a Pt-BMG wavy structure fabricated by embossing and hot-cutting. The structure is designed in such a way that it can be completely flattened in its elastic region. The maximum strain in the structure is given by $\varepsilon = t/d$, where ε is the strain, $t = 10$ μm is the thickness of the structure, and $d = 700$ μm is the curvature (change) during flattening. The maximum strain during flattening of a wavy structure ($\varepsilon = 1.4\%$) is smaller than the

elastic strain limit of 2% for Zr-BMG. Thus the deformation during bending is elastic, which was experimentally confirmed where the structure was repeatedly flattened. Figure 6g and h shows the SEM images of scalpels and micro-tweezers fabricated from Zr-BMG by embossing at 430°C for 120 s under a load of 15 MPa. Precise replication of the scalpel and micro-tweezer molds was achieved including the scalpel's tip radius of 1 µm. The micro-tweezers were repeatedly tested to grip 100 µm objects. In addition to the hardness, strength, and elasticity of BMGs, which are desirable for the use in surgical tools, BMGs are self-sharpening,[53] which prevents blades from blunting.

The success of a biomaterial in the human body depends on the controlled bulk properties (mechanical as well as a match of tissues at the site of implantation) and the surface properties on the micrometer and nano-scale. The shape and bulk properties of biomaterials should mimic the tissues which they are meant to augment or replace. The surface chemistry and topography of the implant material determine how the host tissues interact with the implant.[54] Therefore, the ability to fabricate complex shapes with a wide range of surface topographies is an important property of a biomaterial. The patterning ability of conventional implants is limited and often needs an additional physical or chemical processing step.[48,51] Bulk metallic glasses, on the other hand, offer a great processing advantage that allows combining the surface patterning and fabrication in a single step. Thereby complex 3-D geometries can be net-shaped with a precisely controllable surface topography in which a desirable and predictable cellular response can be programmed. This would benefit a wide range of, and enable new applications in the field of biomedical implants. For example, synthetic membranes are widely used implants. They are a key part of artificial kidneys to perform the filtering action in a similar way to a natural kidney. The ability to precisely tailor pore size in BMG membranes can be used to selectively filter the waste products from blood.

Another potential application for BMGs can be in fabricating implants for soft tissues such as stents. Stents have led to an increase in long-term patency by preventing collapse of vessels following angioplasty. In addition, development of drug-coated stents has lead to further improvement by delaying and reducing the incidence of restenosis. However, both bare and drug-coated stents have been shown to be associated with complications, suggesting that improvements in design and material could have additional beneficial impact.[55,56] The material creating the stent must be flexible, supportive, capable of expansion, biocompatible, and easily producible. The vast majority of stents are made of a stainless steel framework, which is not completely biocompatible and is associated with high occurrence of restenosis. Ideally, stents should induce minimal injury to vessels following deployment and should not activate coagulation and thrombosis. In addition, it is desirable that they are compliant with the blood vessel biomechanics. Bulk metallic glasses are 3–4 times

Figure 7. Gas forming of BMGs: (a–c) Blow molded BMG articles. $Zr_{44}Ti_{11}Cu_{10}Ni_{10}Be_{25}$ was expanded at 450°C for 30 s under a pressure of 10^5 Pa. Free expansion (a) results in 400% strain[44] while blow molding into a patterned mold cavity can replicate complex features with high precision (b,c). (d, e) Porous $Pd_{43}Ni_{10}Cu_{27}P_{20}$ BMG synthesized according to the method described in Figure 6e. (d) (left) amorphous pre-foam containing about 3 vol.% bubbles (after step 2 in Figure 5e). On the right hand side is the resulting foam which was expanded in the SCLR at 390°C for 220 s resulting in a porous volume fraction of about 80%.[45]

more flexible than materials currently used for stent applications, suggesting enhanced compliance. Our short-term in vivo studies suggest they do not induce excessive tissue injury, but their suitability as a stent material requires more detailed evaluation.

Another possible application of BMGs is in the field of chronic electrode implants. Electrode implants are electronic devices implanted in tissues such as the brain to record electrical pulses or stimulate neurons by electrical pulses. Commonly used electrode materials are silicon, platinum, and gold, constructed in many different shapes. The rigid electrodes have shown limited utilization in long-term neural recording due to poor compliance. Specifically, it is believed that deformation of the soft tissue, slight shift, and micromotion can damage cells in the immediate microenvironment leading to poor electrode performance.[57] The flexible electrodes have difficulty in penetrating the living tissue due to a bending effect which occurs following their removal from the supporting wafer.[58,59] A BMG can be designed in a wide range of shapes with varying flexibility. The high strength-to-modulus ratio of BMGs suggests they will be sufficiently strong to penetrate the living tissues yet have adequate compliance to adjust to micromotion and prevent cell death. Furthermore, the fabrication methods of BMGs can produce different geometries of electrodes in order to study the effect of electrode shape and surface topography on the response of neurons.

BLOW MOLDING

Figure 7 shows some examples of blow molding with $Zr_{44}Ti_{11}Cu_{10}Ni_{10}Be_{25}$ BMG using the method described in Figure 5e. As shown in Figure 7a, $Zr_{44}Ti_{11}Cu_{10}Ni_{10}Be_{25}$ BMG was freely expanded at a temperature of 450°C for 30 s under a pressure of 0.1 MPa (1 atm.) that resulted in a deformation of about 400%. This method can also be used to net-shape thin and large geometries when blow-forming the BMG into a mold, as shown in Figure 7b and c. The ability to custom shape complex large and thin geometries is very useful for facial reconstructive implants, which require strength, elasticity, and precise replication of a custom-shaped mold.

Porous BMGs

A current problem in the orthopedic industry, especially with hip replacement implants, is the large mismatch (about an order of magnitude) between the Young's modulus of the metal implant and that of cortical bone. The much higher stiffness of the metal carries a majority of any applied stresses, creating a stress shielding effect for the more compliant bone and leaving it effectively unstressed. Cortical bone, when left unstressed, resorbs into the body in a process termed as disuse atrophy. This resorption weakens the implant/cortical bone interface and can lead to implant loosening and the eventual need for a painful revision surgery.[60] Metallic foams, which are basically metal–air composites, are one possible solution.[61] The modulus of the foam can be decreased to match bone's modulus by decreasing the density of foam according to

$$E_{foam} \propto \left(\frac{\rho_{foam}}{\rho_{bulk}} \right)^2$$

where E_{foam} is the Young's modulus of the foam, and ρ_{foam} and ρ_{bulk} are the densities of the foam and bulk, respectively.[62] However, the undesirable effect of decreasing density of foam is that its strength also decreases. Metallic glass foams have a much higher strength than conventional metal foams of comparable modulus. This is because of the very high strength-to-modulus ratio of metallic glasses.[63] Recently, a foam synthesis method based on TPF was developed where precise control over the density over a wide range can be achieved.[45] Metallic glass foams created by this method can be tailored precisely to mimic the Young's modulus of the bone while still maintaining sufficient strength. Additionally, the porosity of metallic glass foams could also facilitate the ingrowth of bones after implantation. It was found that a pore size on the order of 1 μm results in the best biocompatibility.[64] The ability to independently vary foam density and pore size[45] suggests that metallic glass foams can be engineered to optimum mechanical properties and foreign body response. Metallic glass foams can be open,[65–67] closed,[68] or somewhere in between[45,46] as per requirement. Some examples of metallic glass foams are depicted in Figure 7d,e.

CONCLUSIONS

Bulk metallic glasses are a promising biomaterial due to their superior mechanical properties and corrosion and wear resistance over currently metallic biomaterials. The in vitro and in vivo results indicate that the BMGs are in general nontoxic to cells and compatible with cell growth and tissue function. Unique about BMGs is that chemistry, atomic structure, and surface topography can all be varied independently and the effect of the individual contribution on the biocompatibility was revealed in this work. TPF-based processing methods for BMG were developed which satisfy the required precision and repeatability to shape intricate geometries used in biomedical applications. The ability to precisely net-shape complex geometries combined in a single processing step with patterning the surface will enable us to program desirable and predictable cellular response into a 3-D biomaterial. In general, from reviewing the processing capabilities and properties, it can be concluded that BMGs are useful for many medical devices and implants.

ACKNOWLEDGEMENTS

We thank Eleni Skokos for assistance with cell culture. This work was supported by National Institute of Health grant GM 072194-01 (to T.R.K.), NSF #0826445 (MPM) grant (J.S), and a Yale Institute of Nanotechnology and Quantum Engineering seed grant.

References

1. E. Baden, "Prosthetic Therapy of Congenital and Aquired Clefts on the Palate: An Historical Essay," *J. Hist. Med. Alld. Sci.,* X (3) (1955), pp. 290–301; doi: 10.1093/jhmas/X.3.290.
2. W.L. Johnson, "Bulk Glass-forming Metallic Alloys: Science and Technology," *MRS Bulletin,* 24 (10) (1999), pp. 42–56.
3. J. Schroers and N. Paton, "Amorphous Metal Alloys Form Like Plastics," *Advanced Materials & Processes,* 164 (1) (2006), pp. 61–63.
4. C.A. Schuh, T.C. Hufnagel, and U. Ramamurty, "Overview No.144—Mechanical Behavior of Amorphous Alloys," *Acta Materialia,* 55 (12) (2007), pp. 4067–4109.
5. M.F. Ashby and A.L. Greer, "Metallic Glasses as Structural Materials," *Scripta Materialia,* 54 (3) (2006), pp. 321–326.
6. A. Inoue, T. Zhang, and T. Masumoto, "Zr-Al-Ni Amor-

phous-Alloys with High Glass-Transition Temperature and Significant Supercooled Liquid Region," *Materials Transactions JIM,* 31 (3) (1990), pp. 177–183.
7. K. Jin and J.F. Loffler, "Bulk Metallic Glass Formation in Zr-Cu-Fe-Al Alloys," *Applied Physics Letters,* 86 (24) (2005), 241909.
8. A. Peker and W.L. Johnson, "A Highly Processable Metallic-Glass—$Zr_{41.2}Ti_{13.8}Cu_{12.5}Ni_{10.0}Be_{22.5}$," *Applied Physics Letters,* 63 (17) (1993), pp. 2342–2344.
9. V. Ponnambalam, S.J. Poon, and G.J. Shiflet, "Fe-Mn-Cr-Mo-(Y,Ln)-C-B (Ln = lanthanides) Bulk Metallic Glasses as Formable Amorphous Steel Alloys," *J. Materials Research,* 19 (10) (2004), pp. 3046–3052.
10. Z.P. Lu et al., "Structural Amorphous Steels," *Physical Review Letters,* 92 (24) (2004), 245503.
11. Q.S. Zhang, W. Zhang, and A. Inoue, "New Cu-Zr-based Bulk Metallic Glasses with Large Diameters of up to 1.5 cm," *Scripta Materialia,* 55 (8) (2006), pp. 711–713.
12. D.H. Xu et al., "Formation and Properties of New Ni-based Amorphous Alloys with Critical Casting Thickness up to 5 mm," *Acta Materialia,* 52 (12) (2004), pp. 3493–3497.
13. X.H. Lin and W.L. Johnson, "Formation of Ti-Zr-Cu-Ni Bulk Metallic Glasses," *J. Applied Physics,* 78 (11) (1995), pp. 6514–6519.
14. A. Inoue et al., "Mg-Cu-Y Amorphous-Alloys with High Mechanical Strengths Produced by a Metallic Mold Casting Method," *Materials Transactions JIM,* 32 (7) (1991), pp. 609–616.
15. N. Nishiyama and A. Inoue, "Supercooling Investigation and Critical Cooling Rate for Glass Formation in P-Cu-Ni-P Alloy," *Acta Materialia,* 47 (5) (1999), pp. 1487–1495.
16. J. Schroers et al., "Gold Based Bulk Metallic Glass," *Applied Physics Letters,* 87 (6) (2005), pp. 061912.
17. J. Schroers and W.L. Johnson, "Highly Processable Bulk Metallic Glass-forming Alloys in the Pt-Co-Ni-Cu-P System," *Applied Physics Letters,* 84 (18) (2004), pp. 3666–3668.
18. C.N. Elias et al., "Biomedical Applications of Titanium and Its Alloys," *JOM,* 60 (3) (2008), pp. 46–49.
19. M.L. Morrison et al., "The Electrochemical Evaluation of a Zr-based Bulk Metallic Glass in a Phosphate-buffered Saline Electrolyte," *J. Biomedical Materials Research Part A,* 74A (3) (2005), pp. 430–438.
20. S. Buzzi et al., "Cytotoxicity of Zr-based Bulk Metallic Glasses," *Intermetallics,* 14 (7) (2006), pp. 729–734.
21. L. Liu et al., "Formation and Biocompatibility of Ni-free $Zr_{60}Nb_5Cu_{20}Fe_5Al$ Bulk Metallic Glass," *Materials Transactions,* 48 (7) (2007), pp. 1879–1882.
22. F. Variola et al., "Improving Biocompatibitity of Implantable Metals by Nanoscale Modification of Surfaces: An Overview of Strategies, Fabrication Methods, and Challenges," *Small,* 5 (9) (2009), pp. 996–1006.
23. T. Waniuk, J. Schroers, and W.L. Johnson, "Timescales of Crystallization and Viscous Flow of the Bulk Glass-forming Zr-Ti-Ni-Cu-Be Alloys," *Physical Review B,* 67 (18) (2003), p. 184203.
24. S.M. Jay et al., "Foreign Body Giant Cell Formation is Preceded by Lamellipodia Formation and Can be Attenuated by Inhibition of Rac1 Activation," *American Journal of Pathology,* 171 (2) (2007), pp. 632–640.
25. W.M. Tian and T.R. Kyriakides, "Thrombospondin 2-null Mice Display an Altered Brain Foreign Body Response to Polyvinyl Alcohol Sponge Implants," *Biomedical Materials,* 4 (1) (2009), p. 015010.
26. T.R. Kyriakides et al., "Mice that Lack the Angiogenesis Inhibitor, Thrombospondin 2, Mount an Altered Foreign Body Reaction Characterized by Increased Vascularity," *Proceedings of the National Academy of Sciences of the United States of America,* 96 (8) (1999), pp. 4449–4454.
27. D.D. Deligianni et al., "Effect of Surface Roughness of the Titanium Alloy Ti-6Al-4V on Human Bone Marrow Cell Response and on Protein Adsorption," *Biomaterials,* 22 (11) (2001), pp. 1241–1251.
28. A. Curtis and C. Wilkinson, "Topographical Control of Cells," *Biomaterials,* 18 (24) (1997), pp. 1573–1583.
29. I. Degasne et al., "Effects of Roughness, Fibronectin and Vitronectin on Attachment, Spreading, and Proliferation of Human Osteoblast-like Cells (Saos-2) on Titanium Surfaces," *Calcified Tissue International,* 64 (6) (1999), pp. 499–507.
30. J.M. Anderson, A. Rodriguez, and D.T. Chang, "Foreign Body Reaction to Biomaterials," *Seminars in Immunology,* 20 (2) (2008), pp. 86–100.
31. T.R. Kyriakides et al., "Altered Extracellular Matrix Remodeling and Angiogenesis in Sponge Granulomas of Thrombospondin 2-null Mice," *American Journal of Pathology,* 159 (4) (2001), pp. 1255–1262.
32. D. Bogdanski et al., "Easy Assessment of the Biocompatibility of Ni-Ti Alloys by in Vitro Cell Culture Experiments on a Functionally Graded Ni-NiTi-Ti Material," *Biomaterials,* 23 (23) (2002), pp. 4549–4555.
33. J. Choi et al., "Calcium Phosphate Coating of Nickel-titanium Shape-memory Alloys, Coating Procedure and Adherence of Leukocytes and Platelets," *Biomaterials,* 24 (21) (2003), pp. 3689–3696.
34. J. Schroers, "The Superplastic Forming of Bulk Metallic Glasses," *JOM,* 57 (5) (2005), pp. 35–39.
35. C.J. Gilbert, R.O. Ritchie, and W.L. Johnson, "Fracture Toughness and Fatigue-crack Propagation in a Zr-Ti-Ni-Cu-Be Bulk Metallic Glass," *Applied Physics Letters,* 71 (4) (1997), pp. 476–478.
36. J. Schroers et al., "Transition from Nucleation Controlled to Growth Controlled Crystallization in $Pd_{43}Ni_{10}Cu_{27}P_{20}$ Melts," *Acta Materialia,* 49 (14) (2001), pp. 2773–2781.
37. J. Schroers, Y. Wu, and W.L. Johnson, "Heterogeneous Influences on the Crystallization of $Pd_{43}Ni_{10}Cu_{27}P_{20}$," *Philosophical Magazine a-Physics of Condensed Matter Structure Defects and Mechanical Properties,* 82 (6) (2002), pp. 1207–1217.
38. A. Wiest et al., "Zr-Ti-based Be-bearing Glasses Optimized for High Thermal Stability and Thermoplastic Formability," *Acta Materialia,* 56 (11) (2008), pp. 2625–2630.
39. J. Schroers et al., "Gold Based Bulk Metallic Glass," *Applied Physics Letters,* 87 (6) (2005), p. 61912.
40. J. Schroers, "On the Formability of Bulk Metallic Glass in its Supercooled Liquid State," *Acta Materialia,* 56 (3) (2008), pp. 471–478.
41. G. Kumar, H.X. Tang, and J. Schroers, "Nanomoulding with Amorphous Metals," *Nature,* 457 (7231) (2009), pp. 868–U128.
42. R. Busch, J. Schroers, and W.H. Wang, "Thermodynamics and Kinetics of Bulk Metallic Glass," *MRS Bulletin,* 32 (8) (2007), pp. 620–623.
43. J. Schroers, Q. Pham, and A. Desai, "Thermoplastic Forming of Bulk Metallic Glass—A Technology for MEMS and Microstructure Fabrication," *J. Microelectromechanical Systems,* 16 (2) (2007), pp. 240–247.
44. J. Schroers et al., "Blow Molding of Bulk Metallic Glass," *Scripta Materialia,* 57 (4) (2007), pp. 341–344.
45. J. Schroers et al., "Synthesis Method for Amorphous Metallic Foam," *J. Applied Physics,* 96 (12) (2004), pp. 7723–7730.
46. M.D. Demetriou et al., "High Porosity Metallic Glass Foam: A Powder Metallurgy Route," *Applied Physics Letters,* 91 (16) (2007), p. 161903.
47. T. Wada et al., "Supercooled Liquid Foaming of a Zr-Al-Cu-Ag Bulk Metallic Glass Containing Pressurized Helium Pores," *Materials Letters,* 63 (11) (2009), pp. 858–860.
48. A. Kurella and N.B. Dahotre, "Review Paper: Surface Modification for Bioimplants: The Role of Laser Surface Engineering," *J. Biomaterials Applications,* 20 (1) (2005), pp. 5–50.
49. J. Tan and W.M. Saltzman, "Topographical Control of Human Neutrophil Motility on Micropatterned Materials with Various Surface Chemistry," *Biomaterials,* 23 (15) (2002), pp. 3215–3225.
50. J. Tan and W.M. Saltzman, "Biomaterials with Hierarchically Defined Micro- and Nanoscale Structure," *Biomaterials,* 25 (17) (2004), pp. 3593–3601.
51. N. Nath et al., "Surface Engineering Strategies for Control of Protein and Cell Interactions," *Surface Science,* 570 (1-2) (2004), pp. 98–110.
52. C.C. Berry et al., "The Influence of Microscale Topography on Fibroblast Attachment and Motility," *Biomaterials,* 25 (26) (2004), pp. 5781–5788.
53. H. Choi-Yim et al., "Quasistatic and Dynamic Deformation of Tungsten Reinforced $Zr_{57}Nb_5Al_{10}Cu_{15.4}Ni_{12.6}$ Bulk Metallic Glass Matrix Composites," *Scripta Materialia,* 45 (9) (2001), pp. 1039–1045.
54. P. Roach et al., "Modern Biomaterials: A Review—Bulk Properties and Implications of Surface Modifications," *J. Materials Science-Materials in Medicine,* 18 (7) (2007), pp. 1263–1277.
55. N. Melikian and W. Wijns, "Drug-eluting Stents: A Critique," *Heart,* 94 (2) (2008), pp. 145–152.
56. T.F. Luscher et al., "Drug-eluting Stent and Coronary Thrombosis—Biological Mechanisms and Clinical Implications," *Circulation,* 115 (8) (2007), pp. 1051–1058.
57. V.S. Polikov, P.A. Tresco, and W.M. Reichert, "Response of Brain Tissue to Chronically Implanted Neural Electrodes," *J. Neuroscience Methods,* 148 (1) (2005), pp. 1–18.
58. S. Takeuchi et al., "3D Flexible Multichannel Neural Probe Array," *J. Micromechanics and Microengineering,* 14 (1) (2004), pp. 104–107.
59. S. Takeuchi et al., "Parylene Flexible Neural Probes Integrated with Microfluidic Channels," *Lab on a Chip,* 5 (5) (2005), pp. 519–523.
60. A. Completo, F. Fonseca, and J.A. Simoes, "Strain Shielding in Proximal Tibia of Stemmed Knee Prosthesis: Experimental Study," *J. Biomechanics,* 41 (3) (2008), pp. 560–566.
61. B.V. Krishna et al., "Engineered Porous Metals for Implants," *JOM,* 60 (5) (2008), pp. 45–48.
62. M.F. Ashby, "The Mechanical Properties of Cellular Solids," *Metallurgical and Materials Transactions A,* 14A (1983), pp. 1755–1769.
63. A.H. Brothers and D.C. Dunand, "Porous and Foamed Amorphous Metals," *MRS Bulletin,* 32 (8) (2007), pp. 639–643.
64. C.E. Campbell and A.F. Von Recum, "Microtopography and Soft Tissue Response," *J. Invest. Surg.,* 2 (1989), pp. 51–74.
65. A.H. Brothers and D.C. Dunand, "Syntactic Bulk Metallic Glass Foam," *Applied Physics Letters,* 84 (7) (2004), pp. 1108–1110.
66. T. Wada and A. Inoue, "Formation of Porous Pd-based Bulk Glassy Alloys by a High Hydrogen Pressure Melting-Water Quenching Method and Their Mechanical Properties," *Materials Transactions,* 45 (8) (2004), pp. 2761–2765.
67. J. Jayaraj et al., "Nanometer-sized Porous Ti-based Metallic Glass," *Scripta Materialia,* 55 (11) (2006), pp. 1063–1066.
68. J. Schroers, C. Veazey, and W.L. Johnson, "Amorphous Metallic Foam," *Applied Physics Letters,* 82 (3) (2003), pp. 370–372.

Jan Schroers, Golden Kumar, and Thomas M. Hodges are with the Department of Mechanical Engineering, Yale University, New Haven, CT; Stephen Chan and Themis R. Kyriakides are with the Departments of Pathology and Biomedical Engineering, Yale University, New Haven, CT. Dr. Schroers can be reached at jan.schroers@yale.edu.